An in-line photonic crystal fibre-based Mach–Zehnder interferometer with temperature compensation

2014 Meas. Sci. Technol. 25 107002

(http://iopscience.iop.org/0957-0233/25/10/107002)

IOP Publishing Measurement Science and Technology
Meas. Sci. Technol. **25** (2014) 107002 (5pp) doi:10.1088/0957-0233/25/10/107002

Technical Design Note

An in-line photonic crystal fibre-based Mach–Zehnder interferometer with temperature compensation

Wenhui Ding[1], Yi Jiang[1], Ran Gao[1], Zhen Wang[1] and Yuewu Liu[2]

[1] School of Optoelectronics, Beijing Institute of Technology, Beijing 100081, People's Republic of China
[2] Key Laboratory for Mechanics in Fluid Solid Coupling Systems, Institute of Mechanics, Chinese Academy of Science, Beijing 100190, People's Republic of China

E-mail: bitjy@bit.edu.cn

Received 9 March 2014, revised 14 July 2014
Accepted for publication 23 July 2014
Published 15 September 2014

Abstract
An in-line photonic crystal fibre-based Mach–Zehnder interferometer (PCF-MZI) with temperature compensation has been proposed and experimentally demonstrated. The in-line PCF-MZI is fabricated by splicing a section of photonic crystal fibre between two single mode fibers. The temperature compensation of the in-line PCF-MZI is realized by using materials with proper thermal expansion coefficients. The device possesses the temperature insensitive feature, and a temperature stability of 1.0 pm $°C^{-1}$ has been experimentally demonstrated with the packaging material of ceramic.

Keywords: fiber optic sensor, Mach–Zehnder interferometer, temperature compensation, photonic crystal fiber

(Some figures may appear in colour only in the online journal)

1. Introduction

Photonic crystal fibre-based Mach–Zehnder interferometers (PCF-MZIs) have attracted great interest due to their unique advantages, including their compact size, low cost, high sensitivity, immunity to electromagnetic interference, and ruggedness even in corrosive and other harsh environments [1–3]. The operating principle of the PCF-MZI is based on inter-modal interference, which is induced by the index difference between the core mode and cladding modes. Recently, many different methods are employed to construct a PCF-MZI, such as long period gratings (LPGs [4–7]), mismatched or misaligned core diameter [8–12], or fibre tapers [13–15]. Similar to other interferometric devices, the characteristics and performance of PCF-MZI-based devices are temperature dependent, which can be utilized as temperature sensors. However, these devices also suffer a significant limitation in actual engineering applications due to their temperature cross-sensitivity. Therefore, it is necessary to investigate the temperature influence on the characteristics and performance of PCF-MZI devices and develop temperature compensation methods. Some PCF-MZI sensors with the active temperature compensation have been developed by forming two waist-enlarged fibre tapers at the splice points [16], writing two long-period gratings (LPGs) in the PCF [17], and cascading a MZI and a LPG [18]. However, these configurations make the sensor fragile and susceptible to damage in engineering applications. On the other hand, many researchers have investigated the temperature compensation method by using various packages. Y M Tu's group developed a temperature-insensitive metal package for the fibre Bragg grating [19]. E B Li's group reported a method of temperature compensation for single-mode–multimode–single-mode (SMS) devices by using materials with a proper coefficient of thermal expansion [20].

In this paper, we propose and experimentally demonstrate an in-line PCF-MZI with temperature compensation.

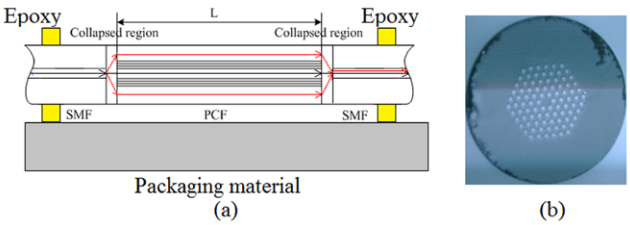

Figure 1. (*a*) Schematic diagram of a PCF-MZI and a structure for its temperature compensation; (*b*) the cross-sectional view of PCF.

The in-line PCF-MZI is fabricated by splicing a section of photonic crystal fibre between two single mode fibres. The temperature dependence of the spectral characteristics of the in-line PCF-MZI is investigated. To overcome the temperature cross-sensitivity of the in-line PCF-MZI, an axial strain, which causes a blue-shift to the transmission spectrum of an in-line PCF-MZI [20], is used to compensate the spectral shift induced by the temperature. Therefore, the in-line PCF-MZI is bonded to a packaging material with a proper thermal expansion coefficient which is higher than that of the PCF, and the temperature compensation of the in-line PCF-MZI can be realized by using the strain which is induced by the thermal expansion of the packaging material. The proposed temperature compensation method is simple, passive, cost effective, and easy to implement.

2. Operation principle

The in-line PCF-MZI shown in figure 1(*a*) is formed by splicing a short piece of index-guiding PCF (YOFC, endless single-mode PCF) between two identical single-mode fibres (Corning, SMF-28). The cross-sectional view of the PCF is shown in figure 1(*b*). The PCF has a pure silica core and a cladding composed of five-ring air holes arranged in a hexagonal pattern. The diameters of the air holes and the entire solid region are 3.75 and 7.5 µm, respectively. The fusion splicing was performed with a commercial fusion splicer (JILONG, KL-260) and the optimum arc current and arc duration for forming a high interferometric visibility were found to be 4.8 mA and 300 ms, respectively. At the fibre splice, a collapsed region is formed between the PCF and the SMF due to strong electric arc discharges. In this configuration, the core mode in the lead-in SMF diffracts to the core and cladding modes of the PCF at the first collapsed region [9]. The two modes propagate alone the PCF with different phase velocity and are recombined in the lead-out SMF fibre at the second collapsed region, forming a Mach–Zehnder interferometer (MZI [21]).

When the external temperature increases, the effective index and the length of the PCF will be changed because of the thermo-optics effect and the thermal expansion. The relative wavelength shift caused by temperature variations can be expressed as [22]

$$\frac{\Delta\lambda_1}{\lambda} = (\alpha_1 + \xi)\,\Delta T \tag{1}$$

where α_1 and ξ are the coefficient of thermal expansion (CTE) and the thermo-optic coefficient of the PCF material, respectively. It can be seen that the transmission spectrum moves to a longer wavelength with the increase of the temperature, and the slope of the temperature dependence is completely determined by the characteristics of the PCF material. Therefore, the temperature can be measured by monitoring the wavelength shift of the peak or dip in the interferometric spectrum.

On the other hand, when an axial strain is applied to an in-line PCF-MZI, the interferomitric spectrum will shift due to the change of fibre dimensions and the photoelastic effect of the fibre. The strain-induced wavelength shift can be expressed as [20],

$$\frac{\Delta\lambda_2}{\lambda} = -\left(1 + 2\nu + p_e\right)\varepsilon \tag{2}$$

where ν is the Poisson ratio of the fibre, p_e is the effective strain-optic coefficient, and ε is the strain applied on the fibre. It is obvious that an axial tensile strain will cause a blue-shift to the transmission spectrum of an in-line PCF-MZI. The spectrum of the in-line PCF-MZI shifts to opposite directions with the temperature and strain. Therefore, the temperature cross-sensitivity of the in-line PCF-MZI can be eliminated by using the strain which is induced by the thermal expansion of a proper packaging material.

The in-line PCF-MZI is bonded to a packaging material with a CTE of α_2, as shown in figure 1. From equation (1), the temperature increase leads to the red-shift for the spectrum of the PCF-MZI. Meanwhile, with the increase of the temperature, an axial tensile strain is induced due to the thermal expansion of the packaging material if the CTE of the packaging material is higher than that of the PCF. The axial tensile strain causes a blue-shift to the transmission spectrum of the in-line PCF-MZI. Therefore, the blue-shift of the spectrum can compensate the red-shift when a proper packaging material is used in the experiment.

When the temperature changes, the axial strain caused by the different CTEs between the PCF and the packaging material is

$$\varepsilon = (\alpha_2 - \alpha_1)\,\Delta T \tag{3}$$

The wavelength shift caused by the temperature variation and axial tensile strain would be

$$\Delta\lambda = \Delta\lambda_1 + \Delta\lambda_2 = \lambda\left[(\alpha_1 + \xi)\,\Delta T - \left(1 + 2\nu + p_e\right)\varepsilon\right] \tag{4}$$

Substituting equation (3) into equation (4) provides

$$\Delta\lambda = \lambda\left[(\alpha_1 + \xi) - (1 + 2\nu + p_e)(\alpha_2 - \alpha_1)\right]\Delta T \tag{5}$$

For an ideal temperature compensation, $\Delta\lambda$ should be zero. With this condition, the CTE of the packaging material can be obtained as

$$\alpha_2 = \alpha_1 + (\alpha_1 + \xi)\,/\left(1 + 2\nu + p_e\right) \tag{6}$$

For silica fibre, $\alpha_1 = 5 \times 10^{-7}\,^{\circ}\mathrm{C}^{-1}$, $\xi = 6.9 \times 10^{-6}\,^{\circ}\mathrm{C}^{-1}$, $p_e = 0.22$, and $\nu = 0.16$. Thus, α_2 of $5.3 \times 10^{-6}\,^{\circ}\mathrm{C}^{-1}$ is calculated. If the CTE of the packaging material is less than α_2, the spectrum of the PCF-MZI will red-shift with the increase in temperature. On the contrary, if the CTE of the packaging

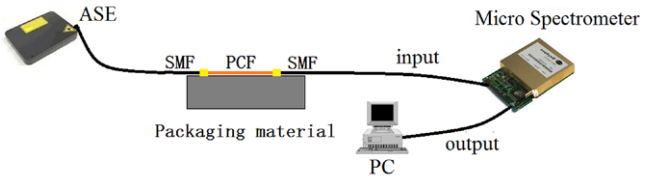

Figure 2. Experimental setup.

material is larger than α_2, the spectrum will blue-shift. In our experiment, three kinds of packaging materials with different CTEs are bonded to the fibre in order to compensate the temperature effect. The temperature stability of the packaged in-line PCF-MZI can be calculated by substituting the CETs of the three materials into equation (5).

3. Experiment

We have tested the temperature feature of the in-line PCF-MZI. The schematic diagram illustrating the mechanism is shown in figure 2. The light source used in this experiment is an amplified spontaneous emission (ASE) broadband source with an output power of 145 mW, and the signal absorption coefficient of the erbium doped fibre is 6 dB m^{-1} at the pump wavelength of 1530 nm. An optical spectrum analyzer (OSA, BaySpec FBGA-F-1525–1565) is used to measure the wavelength shifts. The resolution of the OSA is 115 pm. By using the spline interpolation arithmetic, a wavelength resolution of up to 1 pm can be achieved. Firstly, the in-line PCF-MZI was fabricated with an 8 cm length PCF, and the splicing loss is ~1.2 dB. The MZI loss induced by the splicing and the coupling is measured to be 7.62 dB. The transmission spectrum of the MZI is shown in figure 3. Then, the interferometer was placed into a heating oven and a digital thermometer monitored the internal temperature of the heating oven. Finally, the spectra of the in-line PCF-MZI were recorded by the OSA and the peak wavelengths in the spectra were measured while the heating oven temperatures were changed. Figure 4(*a*) shows the transmission spectra at different temperatures. Obviously, the interference spectrum shifts to the long wavelength when the temperature increases monotonically. In order to obtain the relationship between the resonance wavelength and the temperature, we draw a curve for the wavelength shift of the interference spectra versus temperature, as shown in figure 4(*b*). The wavelength shift increases linearly within the temperature range of 20–140 °C. A linear fitting curve of the experimental data shows an obtained wavelength–temperature sensitivity of 13 pm °C^{-1}.

The axial strain response of the in-fibre PCF-MZI sensor was experimentally investigated. The in-line PCF-MZI with an 8 cm length PCF was attached on a cantilever beam. The axial strain on the cantilever beam was monitored by a strain gauge. The spectra of the in-line PCF-MZI were recorded by the OSA. Figure 5(*a*) shows the transmission spectra with different axial strains. The peak wavelength shifts to the short wavelength with the increase of the axial strain, which agrees with the theoretical analysis. The strain-induced wavelength shift is shown in figure 5(*b*). A linear fitting curve of the

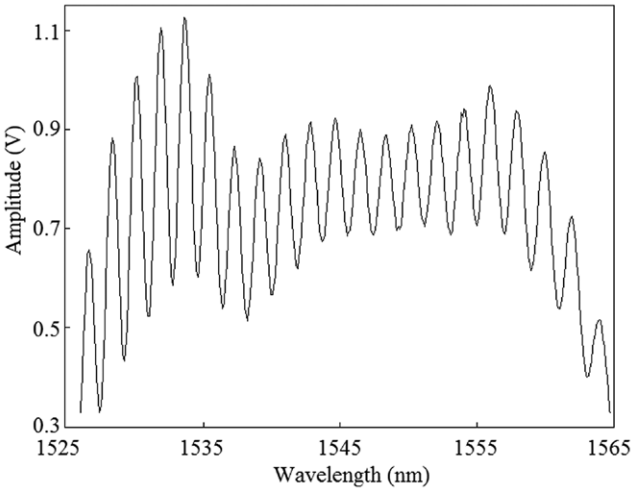

Figure 3. The spectrum of the PCF-MZI.

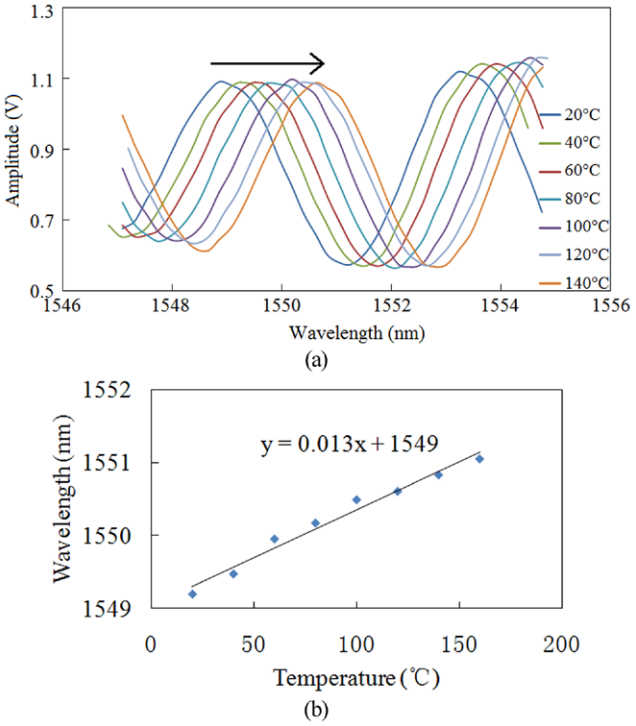

Figure 4. The temperature property of the PCF-MZI: (*a*) the spectrum responses of the in-line PCF-MZI at different temperatures; and (*b*) the relationship between the temperature and the resonance wavelength.

experimental data shows that the wavelength shift is linearly proportional to the axial strain with a sensitivity of 1 pm $\mu\varepsilon^{-1}$. As a consequence of the applied axial strain, two orthogonal linearly polarized modes propagate in the PCF with different propagation constants $\delta\beta$ (birefringence). For silica, the linear-birefringence $\delta\beta$ is proportional to the axial strain, which will lead to the peak wavelength shifting [23]. The peak wavelength shifting caused by the birefringence effect can be calculated to be of the order of 10^{-8} pm [22–24], which is much smaller than our experiment results. Therefore, the birefringence effect is negligible.

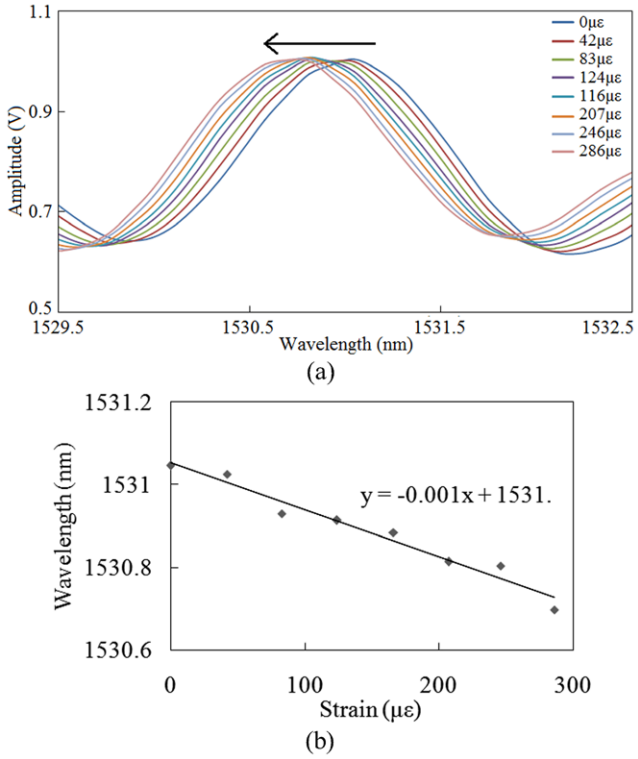

Figure 5. The strain character of the PCF-MZI: (*a*) the output spectrum responses of the in-fibre PCF-MZI with the different strain; and (*b*) the relationship between the strain and the peak wavelength.

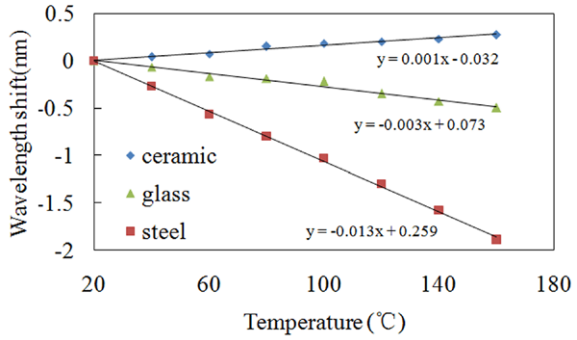

Figure 6. Measured wavelength shifts at different temperatures with three packaging materials.

The proposed temperature compensation method has been experimentally demonstrated. We chose three different packaging materials in experiments, which are steel, glass and ceramic, respectively. Firstly, PCF-MZIs were fabricated and bonded to the three packaging materials by using epoxy resin, as shown in figure 1. Then, we placed the packaged interferometers into the heating oven and recorded the transmission spectra at different temperatures. Figure 6 shows the wavelength shifts at different temperatures for three kinds of packaging material. For the steel package with the CTE of $11 \times 10^{-6}\,°C^{-1}$, the relationship between the temperature and the resonance wavelength can be calculated as $-13.4\,pm\,°C^{-1}$ by using equation (5). In figure 6, the transmission spectrum shifts to the short wavelength, indicating that the CTE of the steel is too

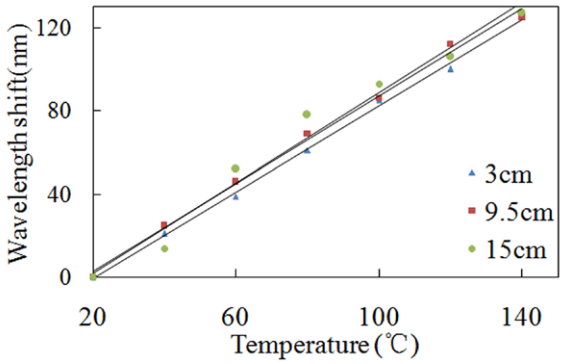

Figure 7. The relationship between the temperature and the wavelength shift with a different length of the PCF.

high to compensate the temperature of the PCF-MZI. The slope of the linear curve fit can be obtained as $-13\,pm\,°C^{-1}$, which agrees with the calculated result of $-13.4\,pm\,°C^{-1}$. For the glass package, a slope of $-3\,pm\,°C^{-1}$ has been experimentally observed, while the calculated slope by using the CTE of the glass ($7.0 \times 10^{-6}\,°C^{-1}$) is $-4.0\,pm\,°C^{-1}$. For the case of the ceramic, a positive slope of $1.0\,pm\,°C^{-1}$ was observed. The ceramic is the most suitable material for the temperature compensation. The temperature sensitivity has been reduced to $1\,pm\,°C^{-1}$ by using the ceramic package, which is more than one order of magnitude lower than the value of $13\,pm\,°C^{-1}$ for the unpackaged PCF-MZI.

We also investigated the relationship between the temperature stability and the length of the ceramic packaged PCF-MZI. PCF-MZIs with different PCF lengths of 3, 9.5, and 15 cm were fabricated and bonded to ceramic packages. Figure 7 shows the relationship between the temperature and the wavelength shift with a different length of the PCF. With the increase of the length of the PCF, the temperature stability of the in-line PCF-MZI with the ceramic package remains substantially unchanged. The temperature stability of the packaged PCF-MZI is determined by the characteristics of the PCF material and the packaging material.

4. Conclusion

In conclusion, we have investigated an in-line PCF-MZI with temperature compensation. The in-line PCF-MZI is fabricated by splicing a section of the PCF between two SMFs. The resonance wavelength in the transmission spectrum of an in-line PCF-MZI, which is induced by temperature and strain, shifts to the opposite direction. Therefore, the temperature compensation of the in-line PCF-MZI can be realized by using materials with a proper coefficient of thermal expansion. Experimental results show that the temperature sensitivity has been reduced to $1\,pm\,°C^{-1}$ by using the ceramic package, which is more than one order of magnitude lower than the value of $13\,pm\,°C^{-1}$ for the unpackaged PCF-MZI. The proposed temperature compensation method is simple, passive, cost effective, and easy to implement.

Acknowledgements

This work is supported in part by Natural Scientific Foundation of China (51075037), Defense Equipments Foundation of China (9140A02060412BQ0101), and National Sci & Tech Key Project (2011ZX05038003).

References

[1] Frazao O, Caldas P, Araújo F M, Ferreira L A and Santos J L 2007 Optical flowmeter using a modal interferometer based on a single nonadiabatic fiber taper *Opt. Lett.* **32** 1974–6
[2] Liu Y and Wei L 2007 Low-cost high-sensitivity strain and temperature sensing using graded-index multimode fibers *Appl. Opt.* **46** 2516–9
[3] Pang F F, Liang W B, Xiang W C, Chen N, Zeng X L, Chen Z Y and Wang T Y 2009 Temperature-insensitivity bending sensor based on cladding-mode resonance of special optical fiber *IEEE Photon. Technol. Lett.* **21** 76–8
[4] Lin C Y, Wang L A and Chern G W 2001 Corrugated long-period fiber gratings as strain, torsion, and bending sensors *J. Lightwave Technol.* **19** 1159–68
[5] Liu Y, Zhang L, Williams J A R and Bennion I 2000 Optical bend sensor based on measurement of resonance mode splitting of long-period fiber grating *IEEE Photon. Technol. Lett.* **12** 531–3
[6] Lim J H, Jang H S, Lee K S, Kim J C and Lee B H 2004 Mach-Zehnder interferometer formed in a photonic crystal fiber based on a pair of long-period fiber gratings *Opt. Lett.* **29** 346–8
[7] Shin W, Ahn T J, Lee Y L, Yu B A and Noh Y C 2010 Highly sensitive strain and bending sensor based on a fiber Mach-Zehnder interferometer in photonic crystal fiber *2010 Conf. on Lasers and Electro-Optics (Cleo) and Quantum Electronics and Laser Science Conference (Qels) (San Jose)* (New York: IEEE)
[8] Choi H Y, Kim M J and Lee B H 2007 All-fiber Mach-Zehnder type interferometers formed in photonic crystal fiber *Opt. Express* **15** 5711–20
[9] Zhou W J, Wong W C, Chan C C, Shao L Y and Dong X Y 2011 Highly sensitive fiber loop ringdown strain sensor using photonic crystal fiber interferometer *Appl. Opt.* **50** 3087–92
[10] Nguyen L V, Hwang D, Moon S, Moon D S and Chung Y J 2008 High temperature fiber sensor with high sensitivity based on core diameter mismatch *Opt. Express* **16** 11369–75
[11] Dong B, Zhou D P, Wei L, Liu W K and Lit J W Y 2008 Temperature- and phase-independent lateral force sensor based on a core-offset multi-mode fiber interferometer *Opt. Express* **16** 19291–6
[12] Dong B, Wei L and Zhou D P 2010 Coupling between the small-core-diameter dispersion compensation fiber and single-mode fiber and its applications in fiber lasers *J. Lightwave Technol.* **28** 1363–7
[13] Tian Z B, Yam S S H, Barnes J, Bock W, Greig P, Fraser J M, Loock H P and Oleschuk R D 2008 Refractive index sensing with Mach-Zehnder interferometer based on concatenating two single-mode fiber tapers *IEEE Photon. Technol. Lett.* **20** 626–8
[14] Lu P, Men L Q, Sooley K and Chen Q Y 2009 Tapered fiber Mach-Zehnder interferometer for simultaneous measurement of refractive index and temperature *Appl. Phys. Lett.* **94** 1093–5 AQ5
[15] Tian Z B and Yam S S H 2009 In-line abrupt taper optical fiber Mach-Zehnder interferometric strain sensor *IEEE Photon. Technol. Lett.* **21** 161–3
[16] Xu F, Li C, Ren D X, Lu L, Lu W W, Feng F and Yu B L 2012 Temperature-insensitive Mach-Zehnder interferometric strain sensor based on concatenating two waist-enlarged fiber tapers *China Opt. Lett.* **10** 070603
[17] Zheng S J, Zhu Y N and Krishnaswamy S 2012 Temperature insensitive all-fiber accelerometer using a photonic crystal fiber long-period grating interferometer *Proc. SPIE* **8347** 83470A
[18] Li T, Dong X Y, Chan C C, Hu L M and Qian W W 2012 Simultaneous strain and temperature measurement based on a photonic crystal fiber modal-interference interacting with a long period fiber grating *Opt. Commun.* **285** 4874–7
[19] Tu Y M, Gong H P, Li S H and Jin Y X 2011 A novel temperature-insensitive package for fiber Bragg grating *Proc. SPIE* **7990** 79900M
[20] Li E 2007 Temperature compensation of multimode-interference-based fiber devices *Opt. Lett.* **32** 2064–6
[21] Villatoro J, Minkovich V P, Pruneri V and Badenes G 2007 Simple all-microstructured-optical-fiber interferometer built via fusion splicing *Opt. Express* **15** 1491–6
[22] Zhang J, Sun H, Rong Q Z, Ma Y, Liang L, Xu Q F, Zhao P, Feng Z Y, Hu M L and Qiao X G 2012 High-temperature sensor using a Fabry-Perot interferometer based on solid-core photonic crystal fiber *China Opt. Lett.* **10** 070607
[23] Islam M S and Mohammad A B 2014 The effect of elastic fatigue on the output transmission of a Mach–Zehnder interferometer comb filter *Opt. Fiber Technol.* **20** 299–302
[24] Ellwood R 2012 The effect of microstructure and fatigue on the acoustoelastic response of aerospace materials *PhD Thesis* University of Nottingham